International Immunopharmacology 71 (2019) 100–108

Contents lists available at ScienceDirect

International Immunopharmacology

journal homepage: www.elsevier.com/locate/intimp

A novel chalcone derivative, L2H17, ameliorates lipopolysaccharide-induced acute lung injury via upregulating HO-1 activity

Yuting Lin[a], Danping Qiu[a], Lili Huang[c], Sangsang Zhang[a], Chenjian Song[a], Beibei Wang[a], Jianzhang Wu[b,*], Chengshui Chen[a,*]

[a] Department of Pulmonary Medicine, The First Affiliated Hospital, Wenzhou Medical University, Wenzhou, Zhejiang 325006, China
[b] Department of Pharmacy, Pharmacy School, Wenzhou Medical University, Wenzhou, Zhejiang 325006, China
[c] Department of Pharmacy, Ningbo Medical Centre Lihuili Hospital, Ningbo, Zhejiang 315041, China

ARTICLE INFO

Keywords:
L2H17
Acute lung injury (ALI)
Lipopolysaccharide (LPS)
Inflammatory responses

ABSTRACT

Background: Chalcone, a natural product, has a wide range of biological activities. L2H17, a chalcone derivative, was synthesized and screened in our previous study and exhibited excellent anti-inflammatory property in vitro. This study investigated the therapeutic potential of L2H17 on lipopolysaccharide (LPS)-induced acute lung injury (ALI) and the role of heme oxygenase-1 (HO-1).

Materials and methods: An ALI animal model was induced by LPS (10 mg/kg) intratracheal instillation. The effect of L2H17 on LPS-induced structural damage was determined using hematoxylin and eosin (HE) staining, and tissue edema extent was examined. Bronchoalveolar lavage fluid (BALF) was harvested to assess the levels of related cytokines by enzyme-linked immunosorbent assay (ELISA), and superoxide dismutase (SOD) activity was also assessed. HO-1 expression was determined using immunohistochemistry and western blotting. The effects of L2H17 on LPS stimulation in RAW 264.7 and the involvement of the HO-1 pathway were investigated.

Results: L2H17 alleviated the histopathological manifestations and tissue edema. Moreover, L2H17 decreased the production of pro-inflammatory factors in BALF and increased SOD activity. In vitro, L2H17 significantly reduced pro-inflammatory cytokine production. Additionally, L2H17 improved the expression of HO-1 in LPS-treated lung tissue and RAW 264.7. We also found that the inhibitory effect of L2H17 on the inflammatory responses was attenuated by an inhibitor of HO-1 activity, Tin protoporphyrin IX (SnPP).

Conclusion: Our data confirmed that L2H17 can exert protective effect on ALI in vitro and in vivo by inhibiting inflammatory responses and modulating the HO-1 pathway.

1. Introduction

Acute lung injury (ALI) is a life-threating condition with a significant mortality rate [1], which results from a wide range of etiologies, including severe respiratory infections, trauma, and acute pancreatitis [2]. This severe respiratory disorder is characterized by alveolar epithelial cell dysfunction followed by capillary permeability, vascular leak, and inflammatory cytokine infiltration, all of which result from the complex inflammatory cascade orchestrated by a variety of pro-inflammatory and anti-inflammatory factors. There is no specific drug therapy to control ALI yet, and drug treatment is limited to adrenocortical hormone. So, there remains an urgent and unmet need to find new drugs with therapeutic potential and explore new targets to treat ALI. Lipopolysaccharide (LPS), a major constituent in the outermost layer of the cytomembrane of Gram-negative bacteria, can trigger diverse infections, such as devastating pneumonia, and may also disturb immune system function [3,4]. Therefore, intratracheal administration of LPS has been widely accepted to develop an ALI animal model in mice [5].

Chalcone is one member of the flavonoid family, widely found in various fruits, vegetables, and beverages. Previous studies have demonstrated that chalcone exerts its potent capability in anti-inflammation, anti-tumor, immunoregulation, and nitric oxide inhibition [6,7]. Our recent studies have indicated that the chalcone derivative, L2H17 [(*E*)-3,4-dihydroxy-2′-methylether ketone] exhibits anti-inflammatory and antioxidant properties in the treatment of renal and cardiac diabetic complications and obesity-related glomerulopathy (ORG) in vivo and in vitro [8,9] by targeting NF-*k*B/MAPK pathways. L2H17 was also reported to inhibit tumor promotion and progression through inactivated NF-kB and protein kinase B (Akt) signaling

* Corresponding authors.
E-mail addresses: wjzwzmu@163.com (J. Wu), chenchengshui@wmu.edu.cn (C. Chen).

https://doi.org/10.1016/j.intimp.2019.02.002
Received 28 October 2018; Received in revised form 2 February 2019; Accepted 3 February 2019
Available online 15 March 2019

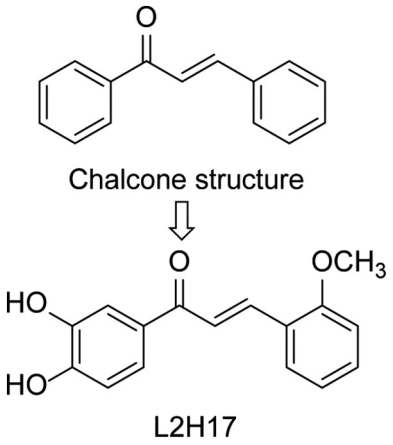

Fig. 1. The molecular structure of L2H17.

pathways [10]. However, whether L2H17 can mitigate acute lung injury remains unknown.

HO-1, known as heme oxygenase-1, is an anti-inflammatory and antioxidant enzyme which plays a pivotal role against airway inflammation by reducing the expression of pro-inflammatory cytokines, such as tumor necrosis factor-α (TNF-α), interleukin-6 (IL-6), and interleukin-1β (IL-1β), and the level of intracellular reactive oxygen species (ROS). ROS accumulation plays a central role in oxidative stress, which results in severe lung inflammation in ALI [11,12].

Collectively, this study investigated the protective potential of L2H17 against ALI in mice and the role played by HO-1 signaling pathway in L2H17's anti-inflammatory effect.

2. Materials and methods

2.1. Reagents

LPS was obtained from Sigma (L2630, LPS from *E. coli* O111:B4). L2H17 was prepared with a purity of 99.2%. The structure of L2H17 is shown in Fig. 1. Superoxide dismutase (SOD) assay kits and Bradford protein assay kits were obtained from Nanjing Jiancheng Bioengineering Institute (Nanjing, China). ROS assay kits were obtained from Beyotime Biotechnology (Shanghai, China). Cytokines (TNF-α, IL-6, and IL-1β) enzyme-linked immunosorbent assay (ELISA) detection kits were provided by Boyun Biotechnology (Shanghai, China). Stain buffer, bovine serum albumin (BSA), Lysing Buffer, CD45-FITC, Ly-6G PerCP-Cy5.5, F4/80 PE, and CD3-AF647 were obtained from BD Biosciences (CA, USA). Anti-HO-1 antibody was from Abcam (Shanghai, China). Tin protoporphyrin IX (SnPP) was purchased from Cayman Chemical (Michigan, USA).

2.2. Animals and model of LPS-induces ALI

Animal care and treatment procedures were carried out in accordance with the protocols of the Institutional Animal Care and Use Committee of Wenzhou Medical University (Wenzhou, China). In total, 50 male C57BL/6 mice (20–24 g) (Experimental Animal Center of Wenzhou Medical University) were housed in groups of 2 to 3 mice under specific pathogen-free (SPF) conditions at temperatures of 22–24 °C with pelleted food and sterile water. They were divided randomly into five groups: (i) control (PBS), (ii) LPS, (iii) L2H17, (iv) LPS + dexamethasone (LPS + Dex), and (v) LPS + L2H17 groups. Dexamethasone was used as a positive comparison. The mice in groups L2H17, LPS + L2H17 and LPS + dexamethasone were intragastrically administered with L2H17 (20 mg/kg) and dexamethasone (2 mg/kg). After the treatment for 6 h, intratracheal instillation of LPS (10 mg/kg) was performed to induce an ALI mice model. Meanwhile, phosphate-buffered saline (PBS) was administered in a similar way to act as a non-inflammatory control. Twenty-four hours after LPS challenge, the bronchoalveolar lavage fluid (BALF) was harvested for further investigation.

2.3. Cell culture

RAW 264.7 mouse macrophages (Cell Bank of the Chinese Academy of Science, Shanghai, China) were cultured in Dulbecco's modified Eagle's medium (DMEM) with 10% fetal bovine serum (FBS) and 1% penicillin-streptomycin solution at 37 °C in incubators containing an atmosphere of 5% CO_2 and 95% air. The cells were treated with different doses of L2H17 (2.5, 5, 10 μg/mL) for 1 h before stimulating with LPS (1 μg/mL) or PBS. After LPS challenge for 12 h, the total cellular RNA and protein were extracted for real-time quantitative polymerase chain reaction (qPCR) and western blot, respectively. To further illustrate the role of L2H17 in the expression of HO-1, the group of L2H17 alone (5 μg/mL) was also established. Moreover, in some experiments, HO-1 inhibitor SnPP was added to cells at a dose of 20 μg/mL 30 min prior to L2H17 administration.

2.4. Histologic examination

After LPS challenge for 24 h, the mice were sacrificed and the lungs were removed and washed with PBS. Each lung tissue sample was fixed in 10% paraformaldehyde overnight, and paraffin-embedded sections were stained with hematoxylin and eosin (H&E). Inflammatory cell infiltration, vascular congestion, and thickened alveolar walls were observed.

2.5. Lung edema measurement

After appropriate treatments, each lung was removed from the thoracic cavity with trachea and esophagus separated and immediately weighed to determine wet weight. Subsequently, the lung tissues were dehydrated and dried for 24 h at 60 °C before the dry weight was recorded, and the wet/dry weight ratio was calculated to show tissue edema content.

2.6. Collection of BALF

Twenty-four hours post LPS challenge, all animals were euthanized with 4% chloral hydrate and exsanguinated by eyeball extraction. Then, collection of BALF was performed through trachea cannula, and lungs were gently lavaged back and forth 3 times with 0.8 mL PBS. Collected BALF were centrifuged at 12,000 rpm for 15 min at 4 °C. The supernatant was obtained and the level of TNF-α, IL-6, and IL-1β was determined by specific ELISA detection kits.

2.7. Fluorescence-activated cell sorter (FACS) analysis

To examine the leukocyte subsets in BALF, collected samples were centrifuged at 12,000 rpm for 15 min at 4 °C, and the cell pellet was suspended in BSA. The cell suspension was taken for centrifugation at 300*g* for 15 min at 4 °C, and washed twice. One hundred microliters of cell suspension were transferred to a 12 * 75 mm polypropylene test tube. After red blood cell lysis with lysing buffer, cells were incubated with each individual antibody for 20 min at 4 °C in the dark. To identify the total amount of leukocytes, FITC-CD45 was used. Ly-6G PerCP-Cy5.5, F4/80 PE, and CD3-AF647 were used respectively to examine neutrophils, macrophages and T cells. After incubation, the washing procedure was repeated twice with 1 mL of BSA. Samples were then evaluated using a BD LSR II flow cytometer. A minimum of 5000 events were collected for analysis. Each experiment was repeated three times.

2.8. Total protein concentrations in BALF

Total protein concentrations in BALF were measured by using a BCA protein assay kit (Bio-Rad Laboratories). The concentration was determined by measuring the value in the absorbance at 570 nm with a multifunctional microplate reader (Molecular Device, USA).

2.9. Assessments of SOD activity in BALF

BALF was taken for centrifugation at 12,000 rpm for 15 min at 4 °C. Supernatants were collected and analyzed using the SOD kits according to the manufacturer's instruction. SOD activity was calculated based on the optical density readings obtained at 550 nm.

2.10. Immunohistochemical evaluation of HO-1 expression

The level of HO-1 expression of the tissue samples was assessed by immunohistochemistry using the streptavidin-peroxidase method. Rehydrated paraffin sections (3 μm) were treated with 3% H_2O_2 for 30 min, then incubated with normal serum for 20 min at room temperature prior to incubating with anti-HO-1 antibody (1:1000) overnight at 4 °C. Slices were immunostained with the relevant secondary antibody (1:1000) for 1 h at room temperature and washed with PBS. All slices were counterstained with hematoxylin. All the images were captured on an Olympus DP2-TWAIN Image Acquisition System (Tokyo, Japan).

2.11. Real-time quantitative PCR

2×10^6 cells/wall were grown in 12-well plates. The cells were exposed to increasing concentrations of L2H17 (2.5, 5, 10 μM) followed by LPS challenge for 12 h. Lung tissue from each of the five groups was harvested. Total RNA in cells and lung tissues were isolated using Trizol reagent (Invitrogen, Carlsbad, CA) and transcribed into cDNA according to the manufacturer's instructions. The ΔCt method was used to quantify mRNA levels for cytokines (TNF-α, IL-6, and IL-1β), and the housekeeper gene glyceraldehyde 3-phosphate dehydrogenase (GAPDH) was used as a reference. Each sample was run in triplicate. The following primer sequences were: TNF-α (F-GCGACGTGGAACTG GCAGAAG, R-GCCACAAGCAGGAATGAGAAGAGG); IL-6 (F-TCCATCC AGTTGCCTTCTTG, R-AAGCCTCCGACTTGTGAAGTG); IL-1β (F-TCGC AGCAGCACATCAACAAGAG, R-TGCTCATGTCCTCATCCTGGAAGG); HO-1 (F-TCCTTGTACCATATCTACACGG, R-GAGACGCTTTACATAGTG CTGT); and GAPDH (F-AGGTCGGTGTGAACGGATTTG, R-TGTAGACC ATGTAGTTGAGGTCA). Relative mRNA expression values were calculated by the $2^{-\Delta\Delta Ct}$ method [13].

2.12. Cellular protein level of cytokines

To further measure the protein concentration of pro-inflammatory cytokines including TNF-α, IL-6, and IL-1β in vitro, 2×10^6 cells/wall were grown in 6-well plates and exposed to increasing concentrations of L2H17 (2.5, 5, 10 μM) prior the treatment in the presence of PBS or LPS for 24 h. Treated cells were collected and taken for repeated freezing and thawing for cell destruction and release of intracellular substances. After centrifugation at 2000 rpm for 20 min at 4 °C, the supernatant was obtained, and the intracellular protein concentrations of TNF-α, IL-6, and IL-1β were analyzed using mouse TNF-α, IL-6, and IL-1β ELISA kits, respectively. Total protein content was detected by using Bradford protein assay kits. The ratio of protein level was calculated according to the following equation: protein concentration of cytokines/ total protein concentration.

2.13. ROS measurement

Intracellular ROS was assessed by using an ROS assay kit. 2×10^6 cells/wall were grown in 6-well plates. RAW 264.7 cells exposed to different treatments were collected and then washed twice in PBS and stained with dichloro-dihydro-fluorescein diacetate (DCFH-DA, 1:1000 dilution with FBS-free DMEM medium) in a 37 °C humidified incubator for 30 min, then washed in PBS three times. Finally, the fluorescence intensities were assessed using a flow cytometer (Franklin Lakes, NJ, USA).

2.14. Western blot

Lysates of cells and lung-tissue homogenate proteins from mice were separated using 12% SDS/polyacrylamide gels, and proteins were transferred onto a polyvinylidene difluoride (PVDF) membrane. Nonspecific sites were blocked by 1.5-h incubation of the membranes in 8% skim milk at room temperature and followed by incubation with primary antibodies against GAPDH (1:1000 dilution) and HO-1 (1:1000 dilution) overnight at 4 °C. Primary antibodies were washed after several washes with tris-buffered saline with Tween (TBST) and labeled by incubating with horseradish peroxidase-conjugated goat anti-rabbit immunoglobulin IgG (1:5000 dilution) for 1 h at room temperature and then washed with TBST. Immunoreactive bands were visualized by electrochemiluminescence (ECL) and exposed to X-ray film. The resultant film images were analyzed by densitometry using Molecular Analyst software (Biorad Laboratories, Hercules, CA). GAPDH was performed as a loading control.

2.15. Statistical analyses

All data were expressed as means ± SD, and statistical analysis was performed by SPSS software 19.0. P-values of < 0.05 were considered statistically significant. The comparison among groups was assessed by the Mann-Whitney test, and data were presented using GraphPad Prism software ver. 5.0 (La Jolla, CA).

3. Results

3.1. Pretreatment with L2H17 protects against LPS-induced ALI in mice

Histology of the lung tissue was examined by light microscopy to determine structural damage degree from different groups. In comparison with control, lung tissue in the LPS group exhibited marked structural abnormalities, including the inflammatory sequestration into the alveolar airspace, alveolar hyperemia, and thickened alveolar walls. However, in the L2H17-treated and Dex-treated groups, these changes were not evident (Fig. 2A). The lung wet/dry weight ratio was calculated to evaluate the extent of pulmonary edema. The results revealed that exposure to LPS increased the lung wet/dry weight ratio notably, whereas in the control, L2H17, Dex-treated, and L2H17-treated groups, the ratio was significantly reduced ($P < 0.01$) (Fig. 2B). After LPS challenge, the total protein concentration in BALF was significantly higher than that in the control group ($P < 0.01$). In contrast, L2H17 or Dex administered 6 h prior to LPS treatment led to the suppression of protein transudation ($P < 0.01$) (Fig. 2C). As expected, the number of total leukocytes in the BALF was significantly larger in the LPS group in comparison with the control, L2H17, LPS + L2H17, and LPS + Dex groups (Fig. 2D). Among leukocyte subsets, the percentage of neutrophils was notably higher than that of macrophages and T cells in BALF ($P < 0.01$) (Fig. 3).

3.2. L2H17 decreases pro-inflammatory factor production and upregulates SOD activity in BALF

A significant increase in the secreted protein of TNF-α, IL-6, and IL-1β was observed in BALF in the LPS group in comparison with the control group ($P < 0.01$), whereas L2H17 or Dex pretreatment substantially reduced pro-inflammatory cytokines ($P < 0.01$) (Fig. 4A).

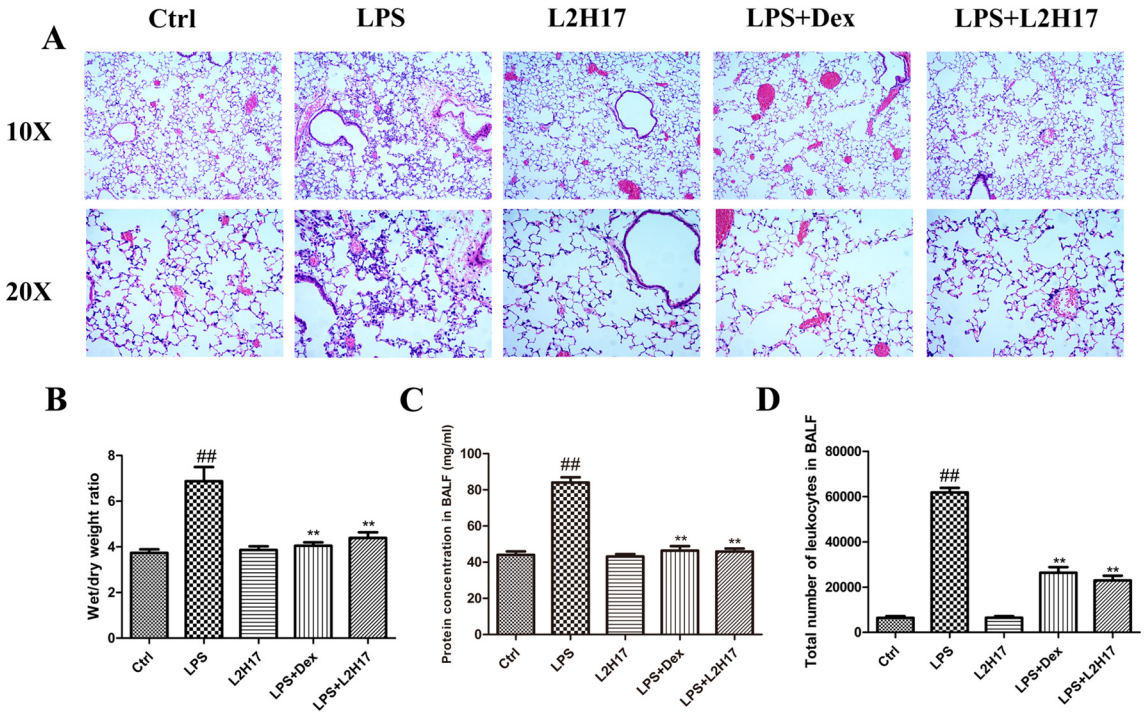

Fig. 2. Protective effects of L2H17 on LPS-induced ALI in mice. (A) Lung histopathological analysis was performed using H&E staining (×10 and ×20) to determine the protective effect on LPS-induced pathological damage. (B) The lung wet/dry weight ratio was determined. (C) Total protein level in BALF was detected using the BSA protein assay kit. (D) The total number of leukocytes in BALF was calculated. Ctrl: control group; LPS: LPS group; L2H17: L2H17 alone group; LPS + Dex: LPS + Dex group; LPS + L2H17: LPS + L2H17 group. The results are presented as means ± SEM (n = 3–6). $^{\#}P < 0.05$, $^{\#\#}P < 0.01$ vs. the control group. $^{*}P < 0.05$, $^{**}P < 0.01$ vs. the LPS group.

SOD activity was increased after L2H17 ($P < 0.05$) or Dex ($P < 0.05$) administration in comparison with the LPS group (Fig. 4B).

3.3. L2H17 upregulates HO-1 expression in vivo

To investigate the effect of L2H17 on HO-1 expression in lung tissue from ALI-induced mice, immunohistochemistry, qPCR, and western blotting were performed to observe the expression of HO-1 in mice lungs 24 h after intratracheal challenge with LPS. The expression of HO-1 in the LPS group was slightly upregulated, but there were no statistically significant differences between the mice in the control group and the mice only treated with LPS. However, there was a statistically significant difference between the control group and the group of L2H17 alone ($P < 0.05$), indicating that L2H17 itself can upregulate the HO-1 expression. Moreover, the HO-1 expression level was significantly upregulated in the LPS + L2H17 ($P < 0.01$) and LPS + Dex groups ($P < 0.01$) in comparison with the control group and the LPS group (Fig. 5A). Consistent with the results in immunohistochemical evaluation, qPCR and western blotting revealed that the level of HO-1 was significantly upregulated after L2H17 or Dex treatment ($P < 0.01$) (Fig. 5B, C).

3.4. L2H17 protects RAW 264.7 against injury induced by LPS

L2H17 exhibited robust inhibitory effects on the production of inflammation-associated factors including TNF-α, IL-6, and IL-1β released from LPS-challenged RAW264.7, and the effects were dose-related ($P < 0.01$) (Fig. 6A, B). Meanwhile, we selected the most efficient concentration (10 μM) to conduct flow cytometry. ROS, an indicator of oxidative stress, showed a significant increase after LPS stimulation in comparison with the control group. However, the effect was inhibited by L2H17 administration (Fig. 6C). According to western blotting, the expression of HO-1 protein level in the LPS group was slightly enhanced in comparison with the control group. However, cells treated L2H17 alone showed a much higher HO-1 protein level than that in the control group ($P < 0.05$). Additionally, LPS + L2H17 administration significantly upregulated the expression of HO-1 protein level over that in the LPS group ($P < 0.01$) (Fig. 6D).

3.5. An inhibitor of HO-1 activity reverses the L2H17-suppressed pro-inflammatory factor production

To further clarify the role played by HO-1 in the LPS-induced inflammation and oxidative stress in vitro, cells were administered with SnPP 30 min prior to L2H17 treatment. The mRNA expression level in the cells treated with SnPP showed abolished effect on the production of L2H17-reduced inflammation-associated factors including TNF-α, IL-6 and IL-1β in RAW264.7 stimulated by LPS (Fig. 7A). The results were consistent with flow cytometry, which showed that cells treated with SnPP could increase L2H17-suppressed intracellular ROS generation (Fig. 7B).

4. Discussion

As a further evaluation of our previous study on the design and synthesis of new chalcone derivatives, this experiment was undertaken to demonstrate that chalcone L2H17 attenuated lung injury by activating HO-1-dependent inhibition of inflammatory factor overproduction in vivo and in vitro.

ALI remains a severe clinical syndrome that exhibits high morbidity and mortality rates. The lack of effective pharmacological therapies remains a concern in routine clinical practice despite remarkable advances in mechanical strategies and fluid management [14]. LPS and other injurious insults have the potential to activate ROS and prompt the generation of TNF-α, IL-6, and IL-1β. Together, these inflammation-associated compounds can result in the initiation, amplification, and perpetuation of the inflammatory process and the resultant lung injury [15,16]. Thus, LPS has been widely used as a method of provoking ALI

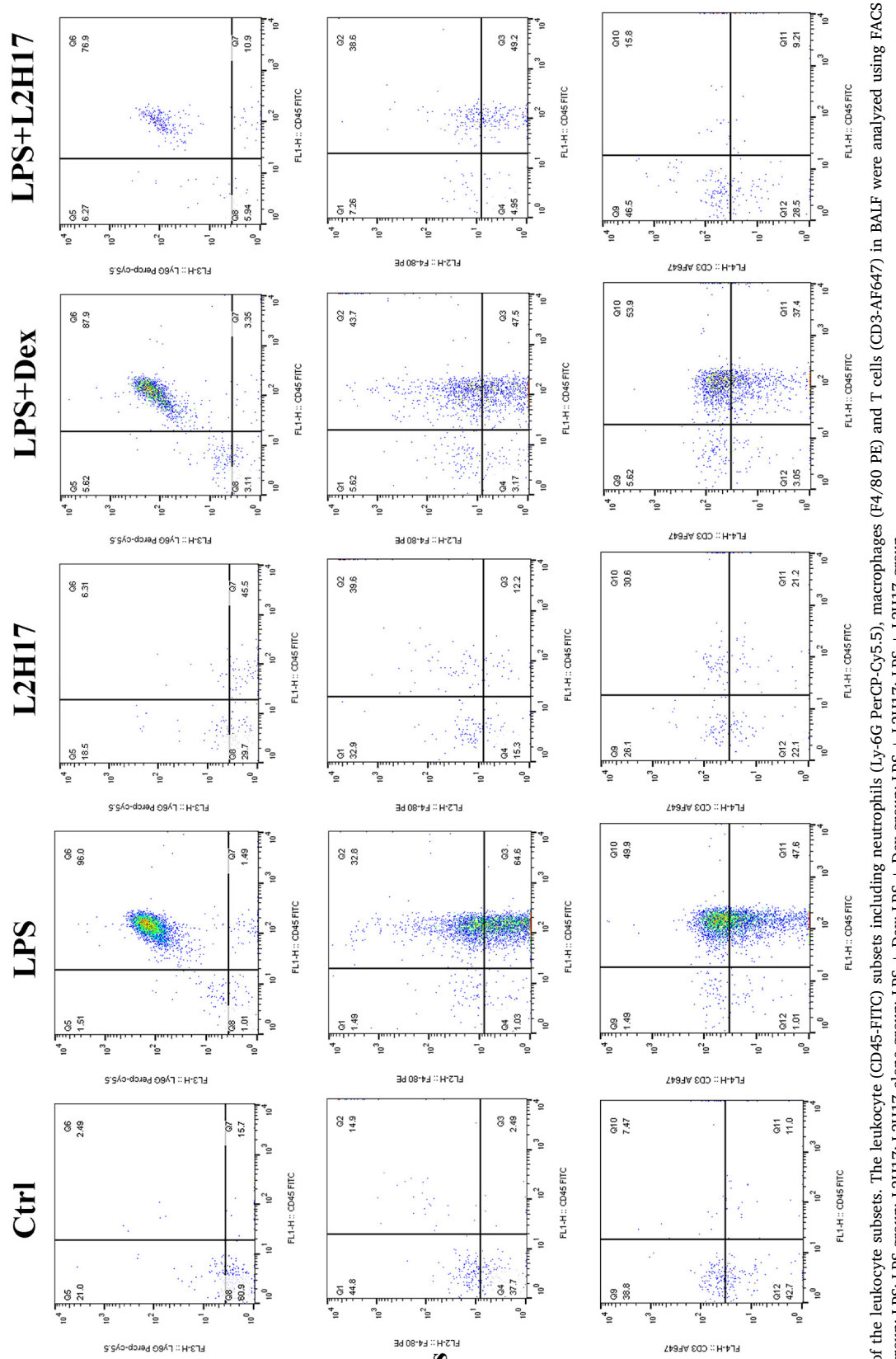

Fig. 3. FACS analysis of the leukocyte subsets. The leukocyte (CD45-FITC) subsets including neutrophils (Ly-6G PerCP-Cy5.5), macrophages (F4/80 PE) and T cells (CD3-AF647) in BALF were analyzed using FACS analysis. Ctrl: control group; LPS: LPS group; L2H17: L2H17 alone group; LPS + Dex: LPS + Dex group; LPS + L2H17: LPS + L2H17 group.

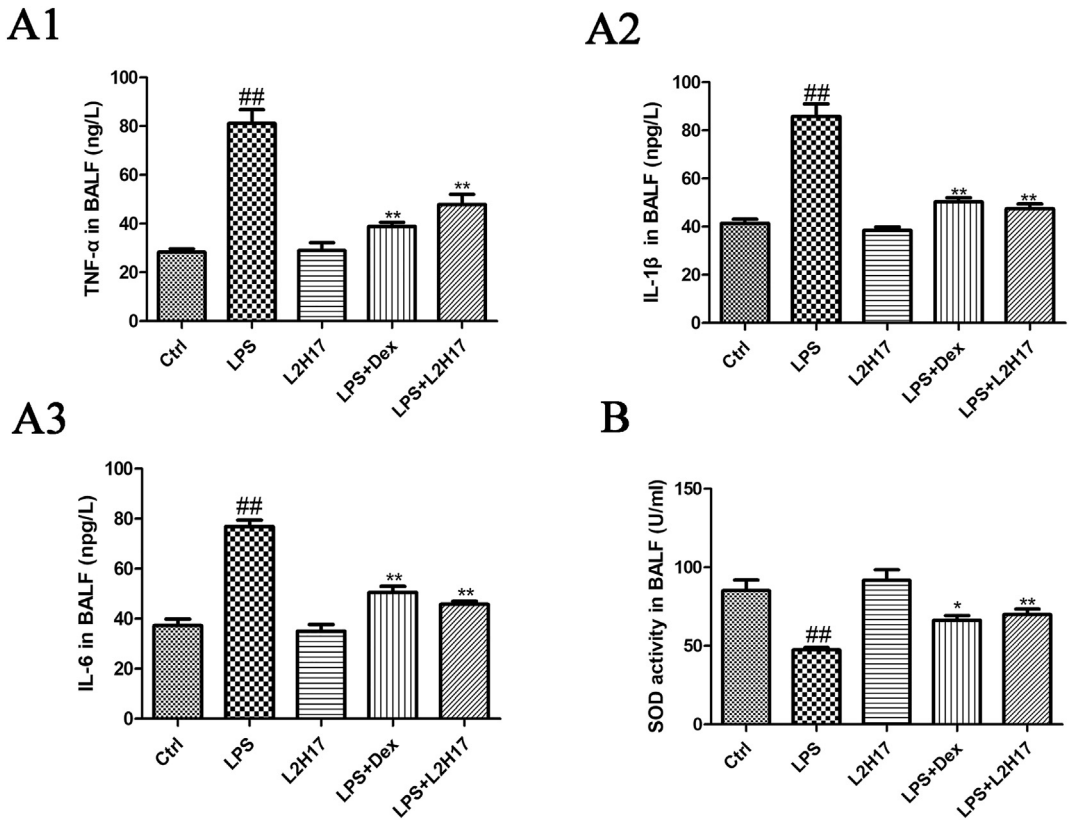

Fig. 4. Anti-inflammatory and antioxidant effects of L2H17 on LPS-induced ALI in mice. The expression of TNF-α (A1), IL-6 (A2), and IL-1β (A3) in BALF was measured by ELISA assay. (B) The SOD activity in BALF was detected. Ctrl: control group; LPS: LPS group; L2H17: L2H17 alone group; LPS + Dex: LPS + Dex group; LPS + L2H17: LPS + L2H17 group. The results are presented as means ± SEM (n = 3–6). $^{\#}P < 0.05$, $^{\#\#}P < 0.01$ vs. the control group. $^{*}P < 0.05$, $^{**}P < 0.01$ vs. the LPS group.

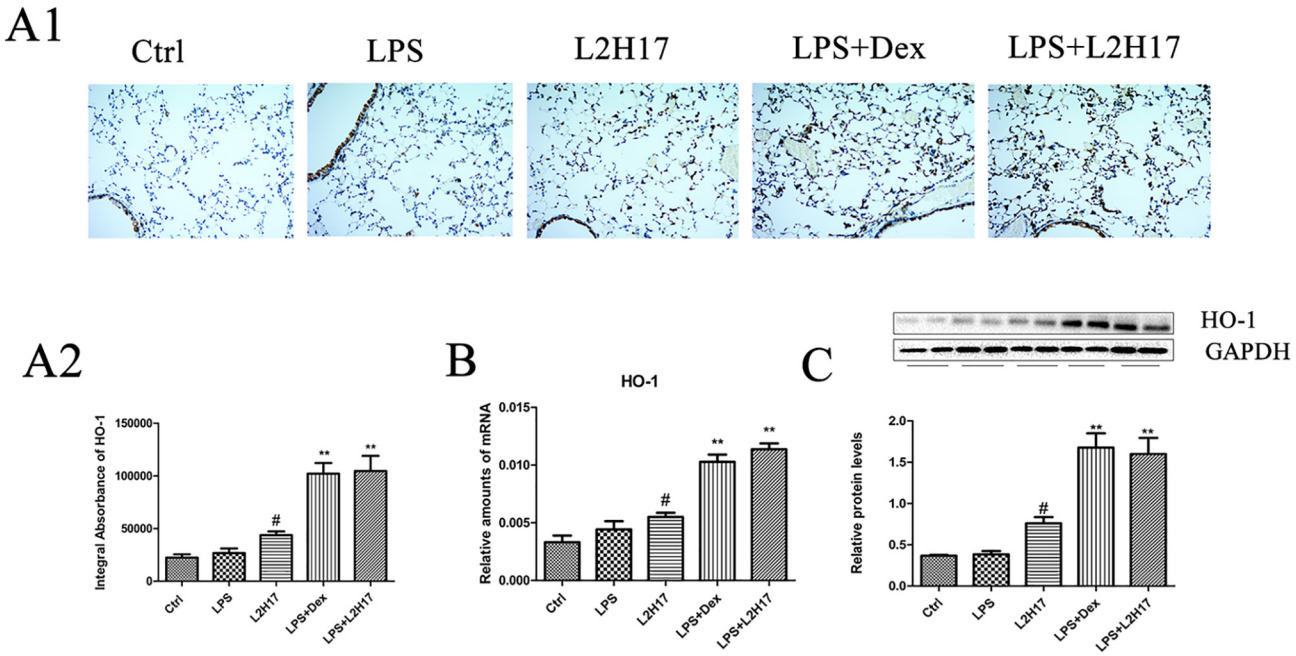

Fig. 5. HO-1 activity was enhanced by L2H17 in LPS-induced ALI in mice. (A) Determination of HO-1 expression level by immunohistochemistry. (B) The mRNA level of HO-1 in lung tissue was measured by qPCR. (C) The protein level of HO-1 in lung extract was detected by western blot analysis. Ctrl: control group; LPS: LPS group; L2H17: L2H17 alone group; LPS + Dex: LPS + Dex group; LPS + L2H17: LPS + L2H17 group. The results are presented as means ± SEM (n = 3–6). Each image is representative of three independent experiments. $^{\#}P < 0.05$, $^{\#\#}P < 0.01$ vs. the control group. $^{*}P < 0.05$, $^{**}P < 0.01$ vs. the LPS group.

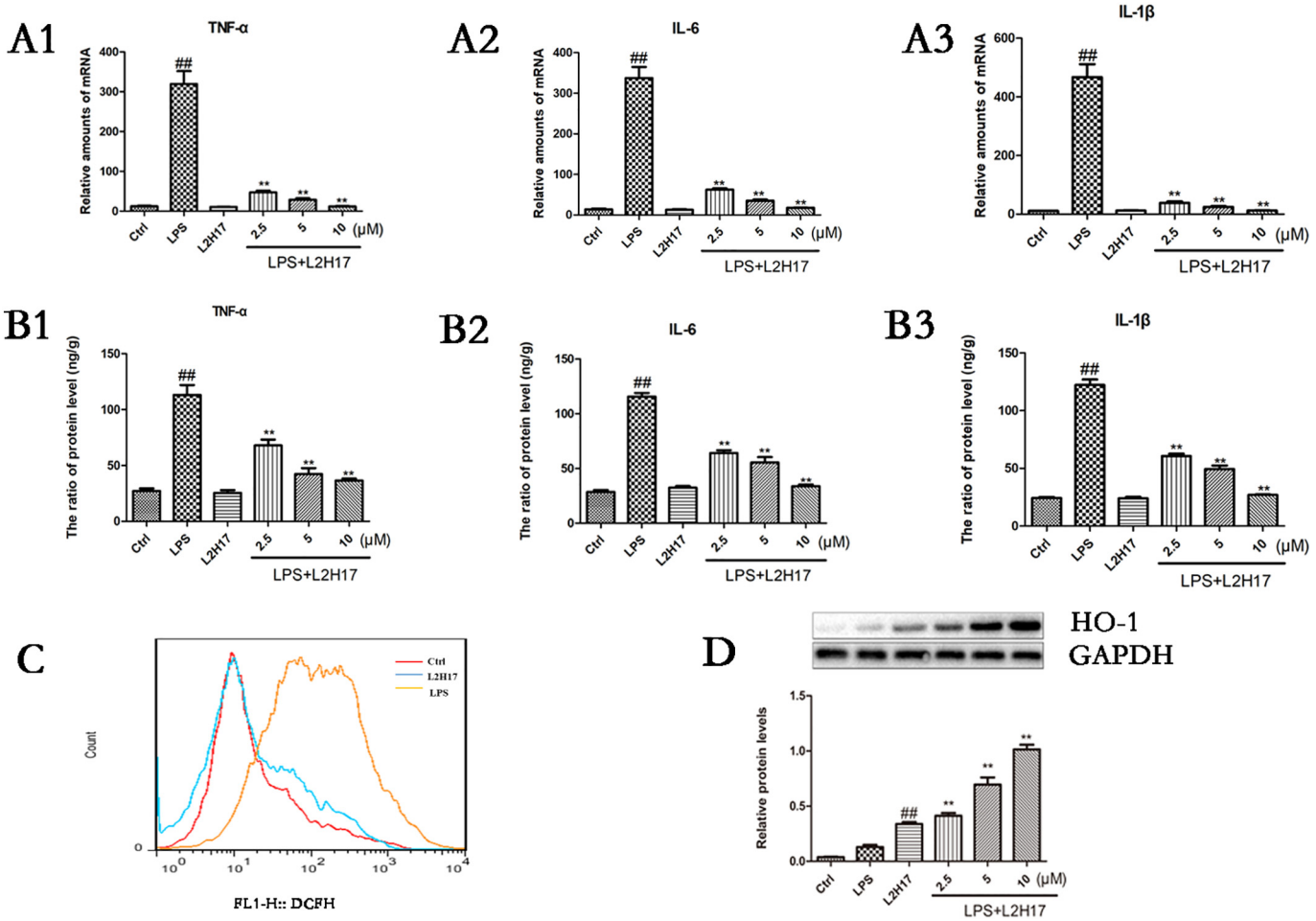

Fig. 6. Suppressive effects of L2H17 on LPS-induced inflammatory and oxidative damage by HO-1 upregulation. The expression of TNF-α (A1), IL-6 (A2), and IL-1β (A3) in cells was measured by qPCR. GAPDH was used as an internal control. (B) The intracellular concentrations of TNF-α (B1), IL-6 (B2), and IL-1β (B3) were measured using ELISA. (C) The most efficient concentration (10 μM) of L2H17 was selected to stimulate cells 1 h prior to LPS administration and the cells were treated in the presence of PBS or LPS for 24 h. Then, the level of ROS was assessed by flow cytometry. (D) The protein expression level of HO-1 in RAW 264.7 cell extracts was assessed. Ctrl represents the control group; LPS represents LPS; L2H17 represents L2H17 (5 μM) alone group; 2.5, 5, and 10 are the L2H17 + LPS treatments groups representing 2.5, 5, and 10 μM, respectively. The results were expressed as means ± SEM from 3 independent experiments. Compared with control: $^{\#}P < 0.05$, $^{\#\#}P < 0.01$; compared with LPS: $^{*}P < 0.05$, $^{**}P < 0.01$.

in experiments. In this study, LPS challenge led to a predominantly alveolar inflammatory lung injury with abnormal changes of histopathologic features of the lungs, overproduction of pro-inflammatory factors and other indicators of inflammatory injury. Based on the fact that neutrophils are responsible for the pathophysiological alterations in the first phase of ALI [17], we also determined the leukocyte subpopulations in BALF. The level of neutrophils was the highest compared to macrophages and T cells according to FACS. The changes described above indicate that mice stimulated with LPS exhibited obvious characteristics of ALI. Chalcones, secondary metabolites of plants and precursors of the flavonoid biosynthesis, have been shown to exert various pharmacological properties [18]. In our previous study, we synthesized and screened some chalcone derivatives. Among them, L2H17 stands out with its excellent antioxidant and anti-inflammatory properties. In our previous studies, L2H17 has been shown to have a protective effect on kidneys with obesity-induced injuries in mice and high glucose-induced injuries in type 1 diabetic mice [8,9]. In this study, mice were pretreated with L2H17 prior to the intratracheal administration of LPS, which ameliorated lung tissue histological changes and inhibited the overproduction of pro-inflammatory factors. In addition, the ratio of lung wet/dry weight, protein leakage, total amount of leukocytes, and neutrophils in BALF were markedly attenuated, indicating that L2H17 blocked the increased capillary permeability and reduced the tissue edema extent. Our in vitro results were consistent with those in vivo, revealing that LPS stimulation caused an increased level of pro-inflammatory cytokines, which was reversed by L2H17 administration in a dose-dependent manner. The generation of ROS is due to incomplete reduction of oxygen within the electron transport chain, and ROS acts as a vital regulator of modification of inflammatory pathways during acute inflammatory process in the lung [19]. Moreover, it has been established that LPS can promote the production of ROS, which has a diverse intracellular signaling cascade [20]. SOD is one of the most important antioxidant enzymes against ROS, which acts as a reflection of the body's capacity to eliminate oxygen free acids [21]. In our study, L2H17 lowered the upregulated SOD enzyme activity in BALF of mice and downregulated ROS production in cells induced by LPS challenge. Therefore, our results supported a beneficial effect of L2H17 in acute LPS-challenged lungs and cells.

As the Nrf2-dependent anti-oxidant gene, HO-1 can decrease the production of harmful heme and produce cytoprotective carbon monoxide (CO) and bilirubin [22,23]. CO, once regarded as a metabolic waste, acts as an anti-inflammatory effector in lung injury in vivo via downregulating the production of pro-inflammatory cytokine. In inflammation and oxidative conditions, upregulation of HO-1 expression shows cell protection capability in a number of lung injury models [24]. In this study, L2H17 reduced the production of inflammation-associated

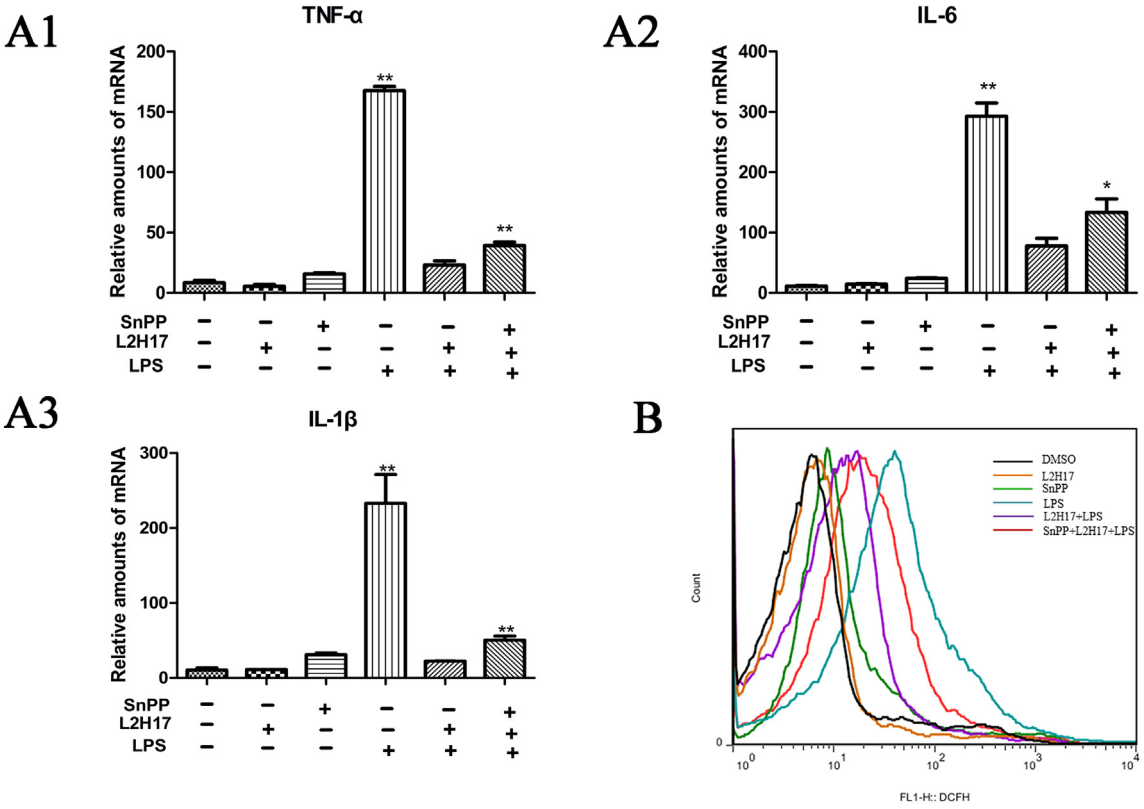

Fig. 7. HO-1 inhibitor reversed the inhibitory effects of L2H17 on LPS-induced pro-inflammatory cytokine production. The mRNA expressions of TNF-α (A1), IL-6 (A2), and IL-1β (A3) were detected by qPCR. (B) The intracellular ROS generation in each group was assessed by flow cytometry. The results were expressed as means ± SEM from 3 independent experiments. Compared with treated with L2H17 and LPS: $^{*}P < 0.05$, $^{**}P < 0.01$.

factors (TNF-α, IL-6, and IL-1β) and ROS level with increasing the level of HO-1 expression significantly. The results are consistent with those reporting that HO-1 could block TNF-α and IL-6 inflammatory mediators [25]. Moreover, pre-treatment with the inhibitor of HO-1 activity (SnPP) was conducted to further confirm whether the anti-inflammatory and anti-oxidative effect of L2H17 was mediated by HO-1. In this study, SnPP inhibited the effect of L2H17 on enhancing HO-1 expression to block the production of TNF-α, IL-6, and IL-1β. These results further indicated that HO-1 may participate the anti-inflammatory effect of L2H17.

5. Conclusion

Our study revealed that L2H17 can act as a therapeutic drug for ameliorating LPS-induced acute lung injury.

Conflict of interest statement

The authors declare no conflicts of interest.

Acknowledgements

The study was supported by the National Natural Science Foundation of China (81570075, 81770074), Zhejiang Provincial Natural Science Foundation (LZ15H010001), and Science and Technology Department of Zhejiang Province (2015103253, 2018264229).

References

[1] D. Qi, X. Tang, J. He, et al., Omentin protects against LPS-induced ARDS through suppressing pulmonary inflammation and promoting endothelial barrier via an Akt/eNOS-dependent mechanism, Cell Death Dis. 7 (9) (2016 Sep 8) e2360.
[2] D.A. Dorward, C.D. Lucas, M.K. Doherty, et al., Novel role for endogenous mitochondrial formylated peptide-driven formyl peptide receptor 1 signalling in acute respiratory distress syndrome, Thorax 72 (10) (2017 Oct) 928–936.
[3] T.R. Martin, Recognition of bacterial endotoxin in the lungs, Am. J. Respir. Cell Mol. Biol. 23 (2) (2000 Aug) 128–132.
[4] Y. Hu, J. Lou, Y.Y. Mao, et al., Activation of MTOR in pulmonary epithelium promotes LPS-induced acute lung injury, Autophagy 12 (12) (2016 Dec) 2286–2299.
[5] K. Takashima, M. Matsushima, K. Hashimoto, et al., Protective effects of intratracheally administered quercetin on lipopolysaccharide-induced acute lung injury, Respir. Res. 15 (2014 Nov 21) 150.
[6] P. Singh, A. Anand, V. Kumar, Recent developments in biological activities of chalcones: a mini review, Eur. J. Med. Chem. 85 (2014 Oct 6) 758–777.
[7] S.N. Bukhari, M. Jasamai, I. Jantan, Synthesis and biological evaluation of chalcone derivatives (mini review), Mini-Rev. Med. Chem. 12 (13) (2012 Nov) 1394–1403.
[8] Q. Fang, J. Wang, L. Wang, et al., Attenuation of inflammatory response by a novel chalcone protects kidney and heart from hyperglycemia-induced injuries in type 1 diabetic mice, Toxicol. Appl. Pharmacol. 288 (2) (2015 Oct 15) 179–191.
[9] Q. Fang, L. Deng, L. Wang, et al., Inhibition of mitogen-activated protein kinases/nuclear factor κB-dependent inflammation by a novel chalcone protects the kidney from high fat diet-induced injuries in mice, J. Pharmacol. Exp. Ther. 355 (2) (2015 Nov) 235–246.
[10] S. Xu, M. Chen, W. Chen, et al., Chemopreventive effect of chalcone derivative, L2H17, in colon cancer development, BMC Cancer 15 (2015 Nov 9) 870.
[11] J.W. Lee, W. Chun, O.K. Kwon, et al., 3,4,5-Trihydroxycinnamic acid attenuates lipopolysaccharide (LPS)-induced acute lung injury via downregulating inflammatory molecules and upregulating HO-1/AMPK activation, Int. Immunopharmacol. 64 (2018 Nov) 123–130.
[12] K. Jiang, S. Guo, C. Yang, et al., Barbaloin protects against lipopolysaccharide (LPS)-induced acute lung injury by inhibiting the ROS-mediated PI3K/AKT/NF-κB pathway, Int. Immunopharmacol. 64 (2018 Nov) 140–150.
[13] T.D. Schmittgen, K.J. Livak, Analyzing real-time PCR data by the comparative C(T) method, Nat. Protoc. 3 (2008) 1101–1108.
[14] D.A. Dorward, J.M. Felton, C.T. Robb, et al., The cyclin-dependent kinase inhibitor AT7519 accelerates neutrophil apoptosis in sepsis-related acute respiratory distress syndrome, Thorax 72 (2) (2017 Feb) 182–185.
[15] M.S. Tsai, Y.H. Wang, Y.Y. Lai, et al., Kaempferol protects against propacetamol-induced acute liver injury through CYP2E1 inactivation, UGT1A1 activation, and attenuation of oxidative stress, inflammation and apoptosis in mice, Toxicol. Lett. 290 (2018 Jun 15) 97–109.
[16] H. Zhang, S. Chen, M. Zeng, et al., Apelin-13 administration protects against LPS-induced acute lung injury by inhibiting NF-κB pathway and NLRP3 inflammasome activation, Cell. Physiol. Biochem. 49 (5) (2018) 1918–1932.

[17] E. Verjans, S. Kanzler, K. Ohl, et al., Initiation of LPS-induced pulmonary dysfunction and its recovery occur independent of T cells, BMC Pulm. Med. 18 (1) (2018 Nov 22) 174.
[18] S. Rocha, D. Ribeiro, E. Fernandes, et al., Systematic review on anti-diabetic properties of chalcones, Curr. Med. Chem. (2018 Oct 1) (Epub ahead of print).
[19] I.S. Chung, J.A. Kim, J.A. Kim, et al., Reactive oxygen species by isoflurane mediates inhibition of nuclear factor κB activation in lipopolysaccharide-induced acute inflammation of the lung, Anesth. Analg. 116 (2) (2013 Feb) 327–335.
[20] L. Chen, P. Liu, X. Feng, et al., Salidroside suppressing LPS-induced myocardial injury by inhibiting ROS-mediated PI3K/Akt/mTOR pathway in vitro and in vivo, J. Cell. Mol. Med. 21 (12) (2017 Dec) 3178–3189.
[21] Y.H. Zhou, J.P. Yu, Y.F. Liu, et al., Effects of Ginkgo biloba extract on inflammatory mediators (SOD, MDA, TNF-alpha, NF-kappaBp65, IL-6) in TNBS-induced colitis in rats, Mediat. Inflamm. 2006 (5) (2006) 92642.
[22] S.W. Chung, X. Liu, A.A. Macias, et al., Heme oxygenase-1-derived carbon monoxide enhances the host defense response to microbial sepsis in mice, J. Clin. Invest. 118 (1) (2008 Jan) 239–247.
[23] L. Bai, W. Shi, J. Liu, et al., Protective effect of pilose antler peptide on cerebral ischemia/reperfusion (I/R) injury through Nrf-2/OH-1/NF-κB pathway, Int. J. Biol. Macromol. 102 (2017 Sep) 741–748.
[24] S.W. Ryter, A.M. Choi, Heme oxygenase-1/carbon monoxide: from metabolism to molecular therapy, Am. J. Respir. Cell Mol. Biol. 41 (3) (2009 Sep) 251–260.
[25] J.F. Luo, X.Y. Shen, C.K. Lio, et al., Activation of Nrf2/HO-1 pathway by Nardochinoid C inhibits inflammation and oxidative stress in lipopolysaccharide-stimulated macrophages, Front. Pharmacol. 9 (2018 Sep 4) 911.